Vascular Pharmacology 113 (2019) 70–76

Contents lists available at ScienceDirect

Vascular Pharmacology

journal homepage: www.elsevier.com/locate/vph

Everolimus depletes plaque macrophages, abolishes intraplaque neovascularization and improves survival in mice with advanced atherosclerosis

Ammar Kurdi[a,1], Lynn Roth[a,1], Bieke Van der Veken[a], Debby Van Dam[b,c], Peter P. De Deyn[b,c,d], Mireille De Doncker[e], Hugo Neels[e], Guido R.Y. De Meyer[a], Wim Martinet[a,*]

[a] Laboratory of Physiopharmacology, Department of Pharmaceutical Sciences, University of Antwerp, Antwerp, Belgium
[b] Laboratory of Neurochemistry and Behaviour, Institute Born-Bunge, University of Antwerp, Antwerp, Belgium
[c] Department of Neurology and Alzheimer Research Center, University of Groningen and University Medical Center Groningen, Hanzeplein 1, 9713, GZ, Groningen, the Netherlands
[d] Department of Neurology, Memory Clinic of Hospital Network Antwerp (ZNA) Middelheim and Hoge Beuken, Lindendreef 1, 2020 Antwerp, Belgium
[e] Laboratory for TDM and Toxicology, ZNA Stuivenberg, Antwerp, Belgium

ARTICLE INFO

Keywords:
mTOR inhibition
Everolimus
Advanced atherosclerosis
Brain hypoxia
Intraplaque neovascularization

ABSTRACT

Background and aims: Inhibition of the mechanistic target of rapamycin (mTOR) is a promising approach to halt atherogenesis in different animal models. This study evaluated whether the mTOR inhibitor everolimus can stabilize pre-existing plaques, prevent cardiovascular complications and improve survival in a mouse model of advanced atherosclerosis.

Methods: $ApoE^{-/-}Fbn1^{C1039G+/-}$ mice ($n = 24$) were fed a Western diet (WD) for 12 weeks. Subsequently, mice were treated with everolimus (1.5 mg/kg daily) or vehicle for another 12 weeks while the WD continued.

Results: Despite hypercholesterolemia, everolimus treatment was associated with a reduction in circulating $Ly6C^{high}$ monocytes (15 vs. 28% of total leukocytes, $p = 0.046$), a depletion of plaque macrophages (2.1 vs. 4.1%, $p = 0.040$) and an abolishment of intraplaque neovascularization, which are all indicative of a more stable plaque phenotype. Moreover, everolimus reduced hypoxic brain damage and improved cardiac function, which led to increased survival (100 vs. 67% of animals, $p = 0.038$).

Conclusions: Everolimus enhances features of plaque stability and counters cardiovascular complications in $ApoE^{-/-}Fbn1^{C1039G+/-}$ mice, even when administered at a later stage of the disease.

1. Introduction

Atherosclerosis is a progressive inflammatory disease of the large and medium-sized arteries and is hallmarked by atherosclerotic plaque formation within the arterial vessel wall. These plaques are end products of lipid accumulation, infiltration of inflammatory cells, smooth muscle cell (SMC) proliferation and matrix formation. Atherosclerotic plaques develop slowly and asymptomatically over the course of decades, but eventually may cause stenosis or thrombotic occlusion of major conduit arteries to the heart and brain, which results in life-threatening complications such as myocardial infarctions and ischemic strokes [1–4]. Despite significant advances in the treatment of cardiovascular diseases, effective prevention of atherosclerosis progression and treatment of its complications remains challenging. Several studies have demonstrated that inhibitors of the mechanistic target of rapamycin (mTOR), such as sirolimus or everolimus, have pleiotropic anti-atherosclerotic effects and that these drugs can be used as add-on therapies to prevent or delay plaque progression [5,6]. However, there is currently a lack of information on the impact of mTOR inhibition on pre-existing atherosclerotic plaques. While there is solid evidence for the anti-inflammatory and anti-proliferative properties of mTOR inhibitors [7,8], the effects of mTOR inhibition on atheroregression, plaque destabilization and plaque-mediated complications, such as myocardial infarction, brain hypoxia and overall survival, have not yet been investigated due to the lack of a suitable animal model presenting these human-like characteristics.

To address these important questions, we determined the effects of the mTOR inhibitor everolimus in a unique model of advanced

* Corresponding author at: Laboratory of Physiopharmacology, University of Antwerp, Universiteitsplein 1, B-2610 Antwerp, Belgium.
E-mail address: wim.martinet@uantwerpen.be (W. Martinet).
[1] Equal contribution.

https://doi.org/10.1016/j.vph.2018.12.004
Received 14 August 2018; Received in revised form 31 October 2018; Accepted 23 December 2018
Available online 24 December 2018
1537-1891/

atherosclerosis: the $ApoE^{-/-}$ fibrillin*(Fbn)1*$^{C1039G+/-}$ mouse model [9, 10]. The heterozygous mutation C1039G$^{+/-}$ in the Fbn1 gene results in fragmentation of elastic fibres in the media of the vessel wall [10]. Combined with a Western diet (WD), degradation of elastic fibres leads to enhanced plaque formation with typical features of human unstable lesions, such as a large necrotic core, high levels of inflammation, intraplaque neovascularization and hemorrhages. Furthermore, $ApoE^{-/-}$ *Fbn1*$^{C1039G+/-}$ mice present human-like complications of advanced atherosclerosis, including myocardial infarctions and brain hypoxia [9, 10]. Our results show that while everolimus is not able to reduce plaque size of pre-existing lesions, it does prevent plaque complexity, which leads to a decrease in atherosclerosis-related clinical manifestations.

2. Methods

2.1.1. Mice

Female $ApoE^{-/-}$*Fbn1*$^{C1039G+/-}$ mice (C57Bl/6 background) were fed a WD (4021.90, AB Diets) starting at an age of 6 weeks. After 12 weeks of WD, the mice were divided into 2 groups receiving either vehicle or everolimus (1.5 mg/kg daily) via osmotic minipumps for another 12 weeks while the WD continued. Everolimus (Novartis Institutes for Biomedical Research) was dissolved in a vehicle consisting of 50% (*v*/v) DMSO, 40% (v/v) propylene glycol and 10% (v/v) absolute ethanol. The mixture was supplemented with 0.4 μl/ml Tween 20. The mice were anesthetized with sevoflurane (8% for induction and 4.5% for maintenance, SevoFlo®, Penlon vaporizer) and subcutaneously implanted with osmotic minipumps (Alzet, model 1004) as previously described [11]. Minipumps were replaced every 4 weeks. The animals were housed in a temperature-controlled room with a 12-h light/dark cycle and had free access to water and food. They were inspected daily for the occurrence of neurological symptoms or sudden death. At the end of the study, blood samples were collected from the retro-orbital plexus of anesthetized mice (ketamine 100 mg/kg, xylazine 10 mg/kg, *i.p.*). Subsequently, mice were sacrificed with sodium pentobarbital (250 mg/kg, *i.p.*). All experiments were approved by the ethics committee of the University of Antwerp (No. 2012–54) and were performed according to the guidelines from Directive 2010/63/EU of the European Parliament on the protection of animals used for scientific purposes.

2.1.2. Plasma cholesterol and everolimus concentrations

Analyses of total plasma cholesterol were performed using a commercially available kit, according to the manufacturer's instructions (Randox). Plasma lipoprotein profiles were determined on pooled samples (60 μl plasma/mouse, 5 mice per measurement) by fast protein liquid chromatography on a Superose 6 column. The plasma concentration of everolimus was determined uisng liquid chromatography tandem mass spectrometry equipped with an online solid-phase extraction, as described previously [11].

2.1.3. Histology

Tissue samples were fixed in 4% formaldehyde (pH 7.4) for 24 h, dehydrated and embedded in paraffin. Serial cross sections (5 μm thick) were prepared for histology. Atherosclerotic plaque size and necrotic core (defined as acellular areas with a threshold of 3000 μm^2) were analyzed on haematoxylin-eosin (H&E) stained sections. The percentage of plaque smooth muscle cells and fibrous cap thickness (median value of 10 measurements per atherosclerotic plaque) was determined on α-SMC actin (F3777, Sigma-Aldrich) stained sections. The percentage of macrophages and proliferative cells was determined via immunohistochemistry using anti-LAMP2 (BD Biosciences, 553,322) and anti-PCNA (Serotec, MCA1558F), respectively. Total collagen content was determined on Sirius red stained sections. To distinguish collagen type I and III in Sirius red stained sections, polarized light microscopy was applied. Apoptosis was determined by immunostaining with anti-cleaved caspase 3 (Cell Signaling, #9661). Intraplaque neovascularization and hemorrhages were examined on H&E stained slides and on slides that were double stained with anti-TER119 (BD Biosciences, 550,565) and anti-vWF (The Binding Site, PC054). Myocardial infarctions (defined as large fibrotic areas with infiltration of inflammatory cells) and perivascular fibrosis, measured as the perivascular collagen area divided by the luminal area (PVCA/LA) of 10 coronary arteries per mouse, were analyzed on Masson's trichrome stained sections. The number of animals showing coronary plaques and the number of coronary arteries with and without plaque in each mouse was evaluated on Masson's trichrome stained transversal sections of the heart (cut from the middle of the heart to the apex).

Analyses of brain hypoxia in the parietal cortex were performed on H&E stained sections. The percentage of pyknotic nuclei was determined as the mean of 3 parietal cortex images per mouse. All images were acquired with Universal Grab 6.1 software using an Olympus BX40 light microscope. Fluorescent images were taken with an EVOS FL Auto Cell Imaging System (ThermoFisher). Staining was quantified using Image J software (National Institutes of Health).

2.1.4. Flow cytometry

EDTA-treated blood (200 μl) was lysed using the red blood cell lysing buffer Hybri-max (Sigma-Aldrich). Thereafter, leukocytes were labelled with the following antibodies (BioLegend): APC anti-CD3ε (145-2C11), PE anti-CD19 (6D5), FITC anti-NK1.1 (PK136), APC anti-Ly6C (HK1.4), PE anti-Gr-1 (RB6-8C5), PerCP anti-CD11b (M1/70), APC anti-CD11c (N418) and FITC anti-I-A^b (KH74). Labelling occurred in the dark at 4 °C in FACS buffer (PBS supplemented with 0.1% BSA and 0.05% NaN3) containing CD16/32 Fc-receptor blocker (BioLegend). Next, cells were analyzed on a BD Accuri C6 cytometer equipped with a blue and red laser (Becton Dickinson). Dead cells were excluded based on forward scatter, side scatter and positive staining for propidium iodide (Invitrogen). Data analysis was performed with FCS Express 4 (De Novo Software).

2.1.5. Echocardiography

Transthoracic echocardiograms were performed on anesthetized mice (sevoflurane; 8% for induction and 4.5% for maintenance, SevoFlo®, Penlon vaporizer) at the start of treatment (12 weeks of WD), at 18 weeks of WD and at the end of the experiment (24 weeks of WD) using a Toshiba diagnostic ultrasound system (SSA-700A) equipped with a 15 MHz transducer. End-diastolic diameter (EDD) and end-systolic diameter (ESD) were measured and fractional shortening (FS = [EDD-ESD]/EDDx100) was calculated.

2.1.6. Motor coordination

Track width was analyzed after 0, 4, 8 and 12 weeks of treatment as described [12]. Briefly, ink was applied to the animal's hind paws and the mice were required to walk on a strip of paper towards a dark goal box. The median value of a minimum of 10 measurements per mouse was used.

2.1.7. Statistical analyses

Normally distributed data are expressed as mean ± SEM and non-normally distributed variables are represented as median [min-max]. Statistical analyses were performed using SPSS software (version 24, SPSS Inc., Chicago). Statistical tests are specified in the figure and table legends. A probability value < 0.05 was considered significant.

3. Results

3.1. Everolimus improves survival of $ApoE^{-/-}$*Fbn1*$^{C1039G+/-}$ mice despite elevated plasma cholesterol levels

$ApoE^{-/-}$*Fbn1*$^{C1039G+/-}$ mice were fed a Western diet (WD) for 12 weeks to induce formation of atherosclerotic plaques. Subsequently,

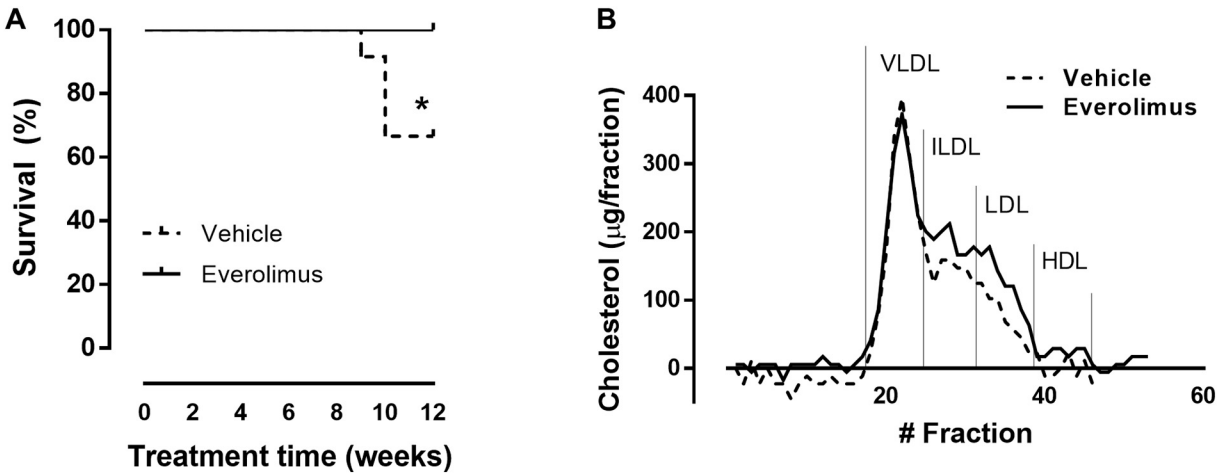

Fig. 1. Everolimus improves survival despite elevated LDL cholesterol levels. (A) Control-treated mice showed a survival rate of 67%, whereas everolimus treatment resulted in 100% survival. *$p < 0.05$ versus vehicle (Log-rank test, $n = 12$ for both groups). (B) Fast protein liquid chromatography was performed on plasma samples (pooled from 5 mice) to determine plasma lipoprotein profile and the result clearly shows an increase in IDL and LDL cholesterol after everolimus treatment.

an osmotic minipump filled with either vehicle or everolimus solution was implanted subcutaneously. The minipump delivered everolimus for 4 weeks at a constant rate of 1.5 mg/kg daily, while the WD was continued. Minipumps were replaced twice to establish a total drug delivery period of 12 weeks. Four out of 12 control animals died abruptly during the experiment, which is a phenomenon that started at 21 weeks of WD (corresponding with 9 weeks of treatment with vehicle solution). Sudden death did not occur in everolimus-treated mice (Log-rank test, $p = 0.038$) (Fig. 1A). Plasma concentrations of everolimus reached 501 ± 58 nM at the time of sacrifice and there was no effect on body weight (data not shown). Further analyses of plasma samples revealed a significant increase in total plasma cholesterol levels in everolimus-treated mice, compared to vehicle-treated controls (576 ± 52 mg/dl vs. 727 ± 34 mg/dl, Student's *t*-test, $p = 0.034$) due to elevated IDL and LDL cholesterol levels (Fig. 1B).

3.2. Everolimus reduces the number of circulating immune cells in $ApoE^{-/-}Fbn1^{C1039G+/-}$ mice

Flow cytometry of circulating blood immune cells showed that everolimus treatment resulted in a significant reduction of several immune cell types including neutrophils, B-cells and ly6C^{high} monocytes (Fig. 2). The percentage of Ly6C^{low} monocytes, dendritic cells, T cells, and natural killer T (NKT) cells was unchanged (Fig. 2).

3.3. Everolimus changes plaque composition in $ApoE^{-/-}Fbn1^{C1039G+/-}$ mice

Despite elevated LDL cholesterol, plaque and necrotic core size was not different in everolimus-treated mice versus controls (Table 1, Fig. S1A). Both macrophage and SMC content were decreased after everolimus treatment (Table 1, Fig. S1B and C). However, the thickness of the fibrous cap did not change (Table 1, Fig. S1C). Total collagen was reduced in plaques of everolimus-treated mice (Table 1, Fig. S1D). Analyses of Sirius red-stained sections under polarized light revealed a significant loss of collagen type III, while collagen type I was unaffected (Table 1, Fig. S1E). Consistent with the anti-proliferative activity of everolimus, the percentage of proliferation cell nuclear antigen (PCNA)-positive cells in everolimus-treated plaques was decreased (Table 1, Fig. S1F).

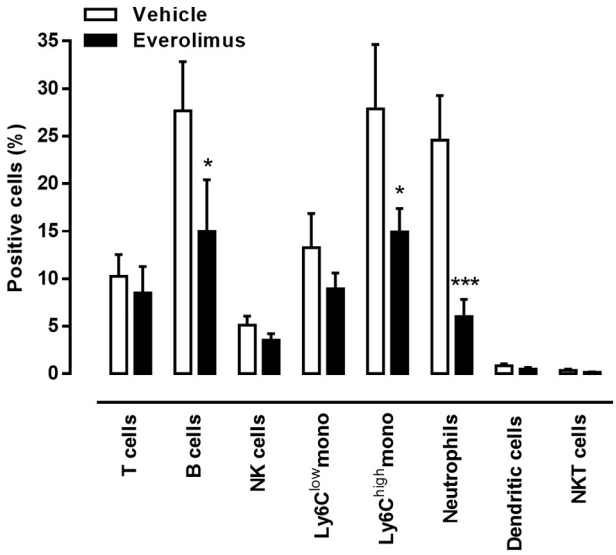

Fig. 2. Everolimus shifts blood immune cells towards a less inflammatory profile in $ApoE^{-/-}Fbn1^{C1039G+/-}$ mice. Blood collected at the moment of sacrifice was processed for flow cytometric analysis of the most important immune cells. *$p < 0.05$; ***$p < 0.001$ versus vehicle (Two-way ANOVA followed by Bonferroni's post-hoc test, $n = 5$ for both groups).

3.4. Everolimus blocks intraplaque neovascularization and hemorrhages in the left common carotid artery of $ApoE^{-/-}Fbn1^{C1039G+/-}$ mice

Intraplaque neovascularization and hemorrhages were examined in longitudinal sections of the left common carotid artery (LCCA). Five of 12 control animals developed microvessels in the LCCA (Fig. 3A). These microvessels appeared to be leaky, as intraplaque hemorrhages were detected using anti-TER119 immunostaining (Fig. 3B). In contrast, none of the everolimus-treated mice showed signs of intraplaque microvessel formation or hemorrhages (Fig. 3A-B).

3.4.1. Everolimus improves cardiac function of atherosclerotic $ApoE^{-/-}Fbn1^{C1039G+/-}$ mice

Treatment with everolimus decreased end systolic diameter (ESD) and increased fractional shortening (FS) as early as 8 weeks after treatment, albeit without changing the end diastolic diameter (EDD) (Fig. 4A). Heart weight over body weight was significantly higher in the control group (1.0 ± 0.1% vs. 0.8 ± 0.1%, Student's *t*-test,

Table 1
Plaque characteristics in *ApoE*$^{-/-}$*Fbn1*$^{C1039G+/-}$ mice after treatment with vehicle or everolimus.

	Vehicle	Everolimus
Plaque size (10^3 µm^2)	752 ± 73	678 ± 119
Necrotic core (%)	7.4 ± 0.9	6.2 ± 1.3
Macrophages (%)	4.1 ± 0.8	2.1 ± 0.4*
Fibrous cap thickness (µm)	8.1 ± 2.3	7.2 ± 2.2
Smooth muscle cells (%)	6.3 ± 0.9	3.6 ± 0.4*
Total collagen (%)	15.9 ± 1.5	8.1 ± 1.2**
Type I collagen (%)	6.0 ± 0.2	4.8 ± 0.6
Type III collagen (%)	2.1 ± 0.4	0.9 ± 0.2*
PCNA positive area (%)	1.1 ± 0.1	0.7 ± 0.1*

Data from proximal ascending aorta, presented as mean ± SEM. All data were analyzed using Student's *t*-test; *$p < 0.05$, **$p < 0.01$ vs. vehicle, $n = 9$–10 per group. PCNA = proliferation cell nuclear antigen. The treatment groups represent data of *ApoE*$^{-/-}$*Fbn1*$^{C1039G+/-}$ mice that received either vehicle or everolimus (1.5 mg/kg daily for 12 weeks) starting at 12 weeks of WD and without discontinuing the WD.

$p = 0.035$). There was no statistical difference in the number of mice with coronary atherosclerosis (8 out of 12 mice in the control group vs. 7 out of 12 mice in the everolimus-treated group, Pearson Chi-square, $p = 0.673$). Furthermore, the number of coronary arteries with atherosclerotic plaques per heart was not changed (control: 1[0–3] vs. everolimus: 1[0–3], Mann-Whitney *U* test, $p = 0.799$). However, hearts in the control group showed more fibrosis both in the myocardium and in the perivascular area around the coronaries (Fig. 4B-C). Signs of myocardial infarction (large infarcted zone) were seen in 2 out of 12 control mice and 3 out of 12 everolimus-treated mice (Pearson Chi-square, $p = 0.615$).

3.5. Everolimus improves motor function and reduces hypoxic damage in the brain of *ApoE*$^{-/-}$*Fbn1*$^{C1039G+/-}$ mice

Because *ApoE*$^{-/-}$*Fbn1*$^{C1039G+/-}$ mice develop neurological symptoms such as head tilt and aberrant motor function (i.e. increased track width) after feeding a WD [12], brains of all treated animals were examined. Hypoxic damage, as shown by pyknotic neurons and eosinophilic cytoplasm, was obvious in the parietal cortex of both vehicle- and everolimus-treated animals (Fig. 5A). However, everolimus led to a significant reduction of pyknotic neurons as compared to controls (37 ± 2.1% vs. 16 ± 1.0%, Student's *t*-test, $p < .001$). Moreover, development of increased track width was inhibited in everolimus-treated mice, suggesting improved motor function (Fig. 5B).

4. Discussion

A large body of evidence suggests that inhibitors of mTOR offer a novel approach to attenuate formation of atherosclerotic plaques [5]. Indeed, mTOR inhibitors such as everolimus significantly reduce the onset of atherogenesis in different animal models [5,13,14], even though little is known about the impact of these drugs on established plaques. In one study focusing on pre-existing lesions of LDL-receptor deficient mice, neither regression nor substantial deceleration of growth was detected after everolimus treatment [15]. The authors concluded that everolimus might exert more anti-atherogenic properties in early stages of atherogenesis than in advanced lesions. It should be noted, however, that LDL-receptor deficient mice are known to develop atherosclerosis, albeit plaque rupture and associated complications such as myocardial infarction and sudden death do not occur and therefore could not be investigated [16]. In the present study, we used a novel animal model of advanced atherosclerosis, namely *ApoE*$^{-/-}$*Fbn1*$^{C1039G+/-}$*mice* [9], to re-evaluate the effects of everolimus on

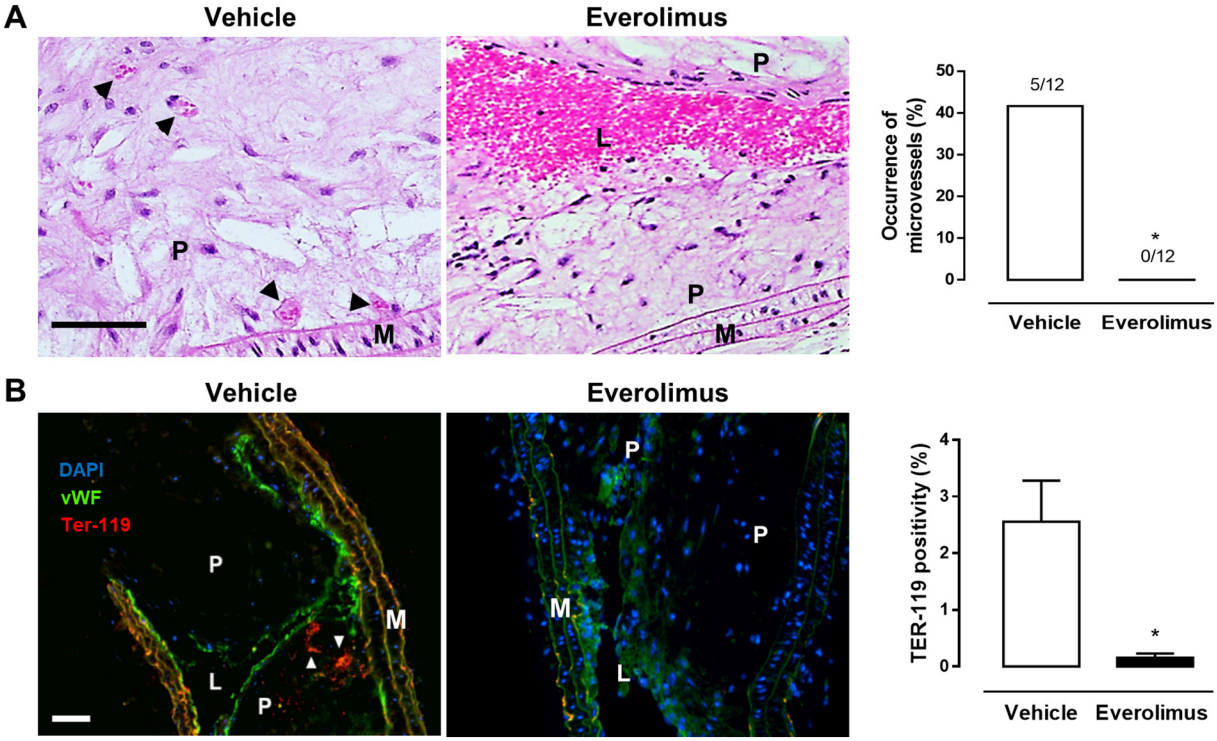

Fig. 3. Everolimus blocks the formation of intraplaque microvessels in the left common carotid artery. (A) Paraffin-embedded, H&*E*-stained atherosclerotic plaques in the left common carotid artery were investigated using light microscopy for the presence of microvessels (arrowheads). *$p < 0.05$ versus vehicle (Pearson Chi-square, $n = 12$ for both groups). (B) Red blood cells indicative of intraplaque hemorrhages and endothelial cells were identified using anti-TER119 and anti-vWF immunostaining, respectively. The percentage of TER119 positivity was quantified. *$p < 0.05$ versus vehicle (Student's *t*-test, $n = 12$ for both groups). Representative images are shown. Scale bar = 100 µm, P = plaque, M = media, L = lumen. (For interpretation of the references to colour in this figure legend, the reader is referred to the web version of this article.)

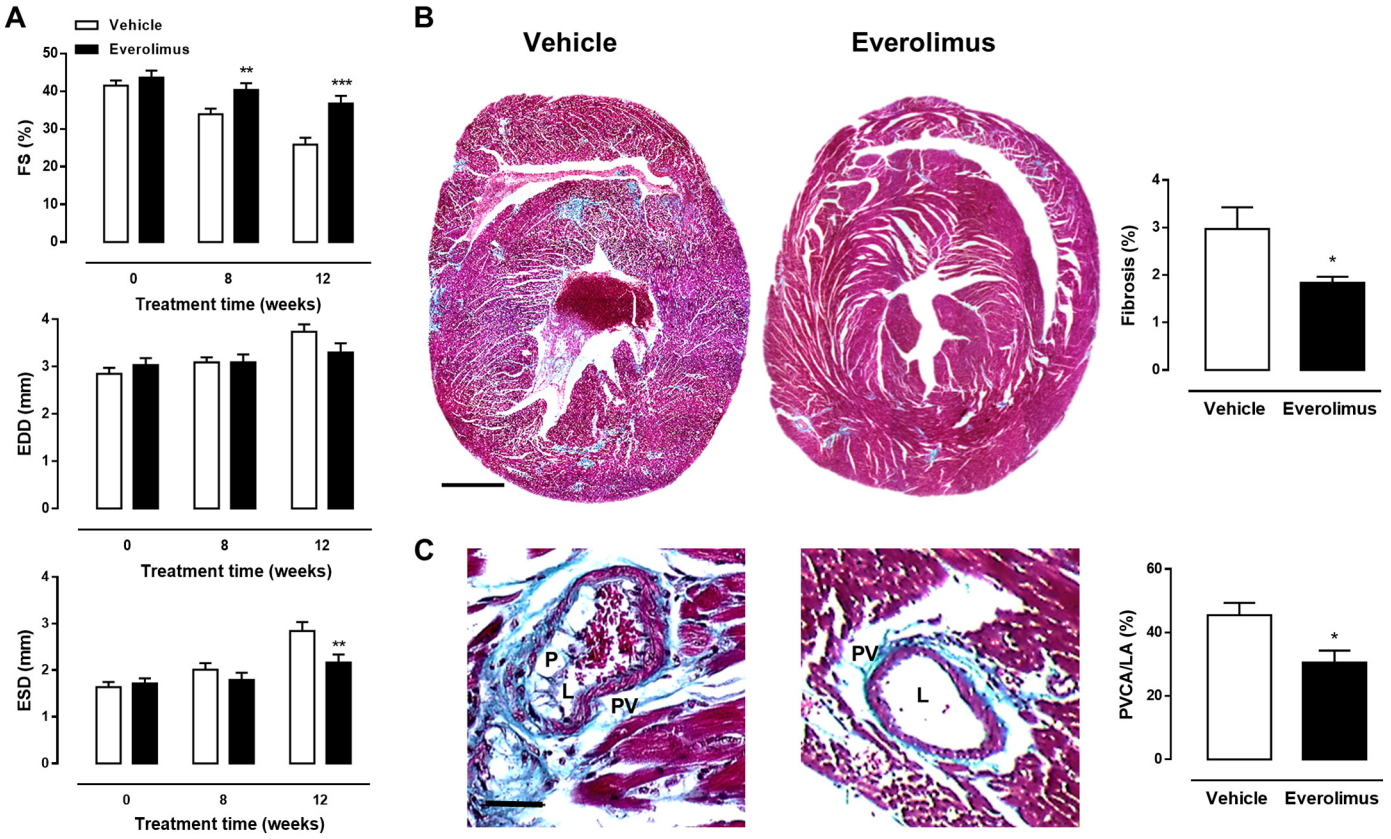

Fig. 4. Everolimus reduces signs of heart failure and myocardial fibrosis in $ApoE^{-/-}Fbn1^{C1039G+/-}$ mice. (A) Echocardiography was performed on anesthetized mice at weeks 0, 8 and 12 of the treatment to assess heart function. FS = fractional shortening, EDD = end diastolic diameter, ESD = end systolic diameter. $^{**}p < 0.01$; $^{***}p < 0.001$ versus vehicle (Two-way ANOVA followed by Bonferroni's post-hoc test, $n = 12$). (B-C) Masson's trichrome staining of heart tissue was performed to evaluate fibrosis (blue area) or presence of coronary plaques and perivascular fibrosis of coronary arteries. PVCA = perivascular collagen area, LA = luminal area, P = plaque, PV = perivascular fibrosis, L = lumen. Scale bar = 500 μm (B) or 100 μm (C). $^{*}p < 0.05$ versus vehicle (Student's t-test, $n = 12$). (For interpretation of the references to colour in this figure legend, the reader is referred to the web version of this article.)

pre-existing lesions and to determine whether everolimus can counter plaque vulnerability and reduce atherosclerosis-driven complications. Given that these complications can be accelerated in $ApoE^{-/-}Fbn1^{C1039G+/-}$ mice via hypertension and mental stress [17,18], or reduced by cholesterol withdrawal and statin therapy [19], this mouse model is a validated and valuable tool for testing pharmacological interventions. To assess the role of mTOR inhibition in attenuating plaque vulnerability, rather than plaque growth, mice received a WD for a period of 12 weeks before starting therapy. Subsequently, everolimus was administered using osmotic minipumps for an additional 12 weeks, while continuing the WD. This approach allowed the formation of established atherosclerotic lesions prior to commencing the treatment.

Importantly, total plasma cholesterol levels increased after everolimus treatment, which was mainly attributed to higher levels of circulating LDL. It is well-known that mTOR inhibitors increase LDL cholesterol by preventing lipid storage, activating lipolysis and downregulating the expression of hepatic LDL receptors [20]. Despite the increased cholesterol, a reduction of circulating neutrophils and Ly6-C^{high} monocytes was observed, which are considered pro-inflammatory leukocytes typically involved in atherogenesis [21,22]. Interestingly, everolimus did not influence the percentage of Ly6Clow monocytes, which are considered anti-inflammatory. The lower number of neutrophils and Ly6Chigh monocytes in the circulation after everolimus treatment could be related to the regulatory role of mTORC1 in myeloid differentiation. Recently it has been reported that disruption of the mTORC1-S6K1-Myc axis in myeloid development, results in a strong reduction of circulating monocytes and neutrophils [23]. Furthermore, it has been shown that everolimus suppresses the development of inflammatory monocytes in bone marrow by downregulating CD115 in a mouse model of abdominal aortic aneurysm [24].

Everolimus treatment did not affect plaque size in the proximal ascending aorta of the $ApoE^{-/-}Fbn1^{C1039G+/-}$ mice, which is in accordance with a previous study using LDL-receptor deficient mice [15]. However, we could observe a significantly lower SMC content in atherosclerotic plaques. This is most likely the result of reduced proliferation, since it has been extensively described that everolimus has an anti-proliferative effect on SMCs [25–27]. Disruption of mTOR signaling also had a profound inhibitory effect on the production of collagen in the plaque. This can be explained by the lower SMC content and the ability of mTOR inhibitors to suppress de novo protein synthesis in SMCs as previously reported [28,29]. Decreased collagen production and SMC content could be disadvantageous for plaque stability [30]. However, everolimus only inhibited the production of the fragile type III collagen and had no effect on the formation of the stable type I collagen. Furthermore, cap thickness was not altered, which is an important indicator for plaque stability. Importantly, macrophage content was reduced, probably owing to the lower levels of circulating Ly6C^{high} monocytes combined with the previous finding that everolimus reduces the chemoattractant-induced migration of monocytes [13]. However, it cannot be excluded that also reduced macrophage proliferation might have contributed to the lower plaque macrophage content. Analysis of plaques in the common carotid artery showed that everolimus abolished the development of intraplaque neovascularization, a well-known feature of advanced atherosclerosis that promotes infiltration of lipids and leukocytes into the plaque [31]. Diminished intraplaque neovascularization could result from everolimus-mediated inhibition of EC

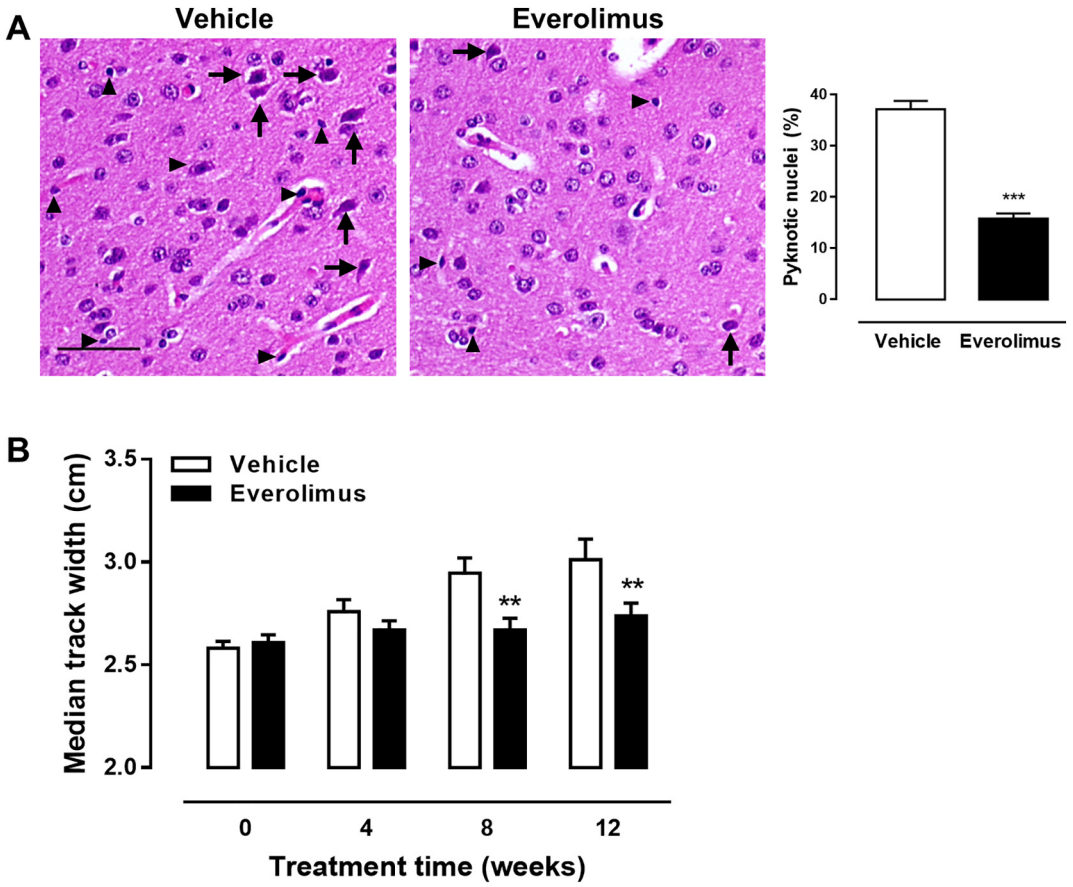

Fig. 5. Everolimus treatment reduces ischemic damage in the parietal cortex of the brain and improves motor function in $ApoE^{-/-}Fbn1^{C1039G+/-}$ mice. (A) Following euthanasia, brains were dissected and fixed in 4% formalin (pH = 7.4). Paraffin embedded brain tissues were stained for H&E and the partial cortex was analyzed under a light microscope for signs of ischemic damage such as pyknotic neurons (arrowheads) and eosinophilic infiltrations (arrows). The percentage of pyknotic nuclei was quantified. Scale bar = 100 μm. $^{***}p < 0.001$ versus vehicle (Student's t-test, n = 5 for both groups). (B) Track width analysis was performed after 0, 4, 8 and 12 weeks of treatment. $^{**}p < 0.01$ versus vehicle (Two-way ANOVA followed by Bonferroni's post-hoc test, n = 12 for both groups).

proliferation [32]. All together, these findings suggest that everolimus promotes features of plaque stability.

The plaque-related effects were accompanied by a reduction of atherosclerosis-driven complications in everolimus-treated mice. Importantly, cardiac function was improved and heart weight was normalized. Moreover, we observed inhibition of total cardiac fibrosis and perivascular fibrosis. It has been reported that mTOR inhibitors are able to reduce cardiac hypertrophy, presumably via reducing arterial stiffness [33]. For instance, everolimus treatment in rats with metabolic syndrome reduced left ventricular hypertrophy and fibrosis [34]. Clinical studies have shown that the use of everolimus suppresses cardiac hypertrophy and improves cardiac function in heart transplant patients [35] as well as in kidney transplant recipients [33,36]. We also investigated the effects of everolimus treatment on cerebral complications by measuring track width at different timepoints. Previous research in $ApoE^{-/-}Fbn1^{C1039G+/-}$ mice validated track width measurement as a method to evaluate hypoxic brain damage in a non-invasive way [12]. Normally, due to brain hypoxia, $ApoE^{-/-}Fbn1^{C1039G+/-}$ mice on a WD try to compensate for a loss in balance by widening the distance between the left and right hind paw, but everolimus reduced the gradual increase in track width over time, indicative of less brain damage. This effect was confirmed via measurement of the pyknotic nuclei in the parietal cortex, showing a lower percentage of pyknosis in the everolimus-treated mice.

Strikingly, everolimus improved survival from 67% to 100%, which is a new and important finding that underscores the potential of mTOR inhibitors for the treatment of cardiovascular disease. However, the exact cause of mortality in the $ApoE^{-/-}Fbn1^{C1039G+/-}$ mouse model is still unknown. The current study strongly suggests that brain hypoxia or heart-related problems are important contributors, since we observed an improved cardiac function and reduced brain hypoxia in the everolimus-treated mice together with a reduced mortality.

Based on the findings described above, we show for the first time that everolimus is able to enhance features of atherosclerotic plaque stability in pre-existing lesions, by impairing recruitment of inflammatory cells (due to a shift of the blood immune cells towards a less inflammatory profile), inhibiting intraplaque neovascularization and suppressing cellular proliferation. Accordingly, atherosclerosis-driven complications such as cardiac hypertrophy and fibrosis, brain hypoxia and sudden death were largely prevented. These results acknowledge the ability of mTOR inhibitors to counter atherosclerosis via multiple routes despite hypercholesterolemia.

Conflict of interest

None declared.

Financial support

This work was supported by the Fund for Scientific Research (FWO)-Flanders (grant numbers G044312N, G016013N) and the University of Antwerp (BOF).

Acknowledgements

The authors thank Bronwen Martin for critically reviewing the

manuscript and Rita Van Den Bossche, Hermine Fret, Anne-Elise Van Hoydonck, and Sanne Lauryssen for their excellent technical support.

Appendix A. Supplementary data

Supplementary data to this article can be found online at https://doi.org/10.1016/j.vph.2018.12.004.

References

[1] C. Weber, H. Noels, Atherosclerosis: current pathogenesis and therapeutic options, Nat. Med. 17 (11) (2011) 1410–1422.
[2] P. Libby, Mechanisms of acute coronary syndromes and their implications for therapy, N. Engl. J. Med. 368 (21) (2013) 2004–2013.
[3] A.J. Lusis, Atherosclerosis, Nature 407 (6801) (2000) 233–241.
[4] S. Yla-Herttuala, J.F. Bentzon, M. Daemen, E. Falk, H.M. Garcia-Garcia, et al., Stabilization of atherosclerotic plaques: an update, Eur. Heart J. 34 (42) (2013) 3251–3258.
[5] A. Kurdi, G.R. De Meyer, W. Martinet, Potential therapeutic effects of mTOR inhibition in atherosclerosis, Br. J. Clin. Pharmacol. 82 (5) (2016) 1267–1279.
[6] W. Martinet, H. De Loof, G.R. De Meyer, mTOR inhibition: a promising strategy for stabilization of atherosclerotic plaques, Atherosclerosis 233 (2) (2014) 601–607.
[7] L. Zhao, T. Ding, T. Cyrus, Y. Cheng, H. Tian, et al., Low-dose oral sirolimus reduces atherogenesis, vascular inflammation and modulates plaque composition in mice lacking the LDL receptor, Br. J. Pharmacol. 156 (5) (2009) 774–785.
[8] W.Q. Chen, L. Zhong, L. Zhang, X.P. Ji, M. Zhang, et al., Oral rapamycin attenuates inflammation and enhances stability of atherosclerotic plaques in rabbits independent of serum lipid levels, Br. J. Pharmacol. 156 (6) (2009) 941–951.
[9] C. Van der Donckt, J.L. Van Herck, D.M. Schrijvers, G. Vanhoutte, M. Verhoye, et al., Elastin fragmentation inatherosclerotic mice leads to intraplaque neovascularization, plaque rupture, myocardial infarction, stroke, and sudden death, Eur. Heart J. 36 (17) (2015) 1049–1058A.
[10] J.L. Van Herck, G.R.Y. De Meyer, W. Martinet, C.E. Van Hove, K. Foubert, et al., Impaired fibrillin-1 function promotes features of plaque instability in apolipoprotein E-deficient mice, Circulation 120 (24) (2009) 2478–2487.
[11] A. Kurdi, M. De Doncker, A. Leloup, H. Neels, J.P. Timmermans, et al., Continuous administration of the mTORC1 inhibitor everolimus induces tolerance and decreases autophagy in mice, Br. J. Pharmacol. 173 (2016) 3359–3371.
[12] L. Roth, D. Van Dam, C. Van der Donckt, D.M. Schrijvers, K. Lemmens, et al., Impaired gait pattern as a sensitive tool to assess hypoxic brain damage in a novel mouse model of atherosclerotic plaque rupture, Physiol. Behav. 139 (2015) 397–402.
[13] R. Baetta, A. Granata, M. Canavesi, N. Ferri, L. Arnaboldi, et al., Everolimus inhibits monocyte/macrophage migration in vitro and their accumulation in carotid lesions of cholesterol-fed rabbits, J. Pharmacol. Exp. Ther. 328 (2) (2009) 419–425.
[14] M.A. Mueller, F. Beutner, D. Teupser, U. Ceglarek, J. Thiery, Prevention of atherosclerosis by the mTOR inhibitor everolimus in LDLR−/− mice despite severe hypercholesterolemia, Atherosclerosis 198 (1) (2008) 39–48.
[15] F. Beutner, D. Brendel, D. Teupser, K. Sass, R. Baber, et al., Effect of everolimus on pre-existing atherosclerosis in LDL-receptor deficient mice, Atherosclerosis 222 (2) (2012) 337–343.
[16] B.E. Veseli, P. Perrotta, G.R.A. De Meyer, L. Roth, C. Van der Donckt, et al., Animal models of atherosclerosis, Eur. J. Pharmacol. 816 (2017) 3–13.
[17] L. Roth, M. Rombouts, D.M. Schrijvers, K. Lemmens, G.W. De Keulenaer, et al., Chronic intermittent mental stress promotes atherosclerotic plaque vulnerability, myocardial infarction and sudden death in mice, Atherosclerosis 242 (1) (2015) 288–294.
[18] L. Roth, D.M. Schrijvers, W. Martinet, G.R. De Meyer, Angiotensin II increases coronary fibrosis, cardiac hypertrophy and the incidence of myocardial infarctions in ApoE$^{-/-}$Fbn1$^{C1039G+/-}$ mice, Acta Cardiol. 71 (4) (2016) 483–488.
[19] L. Roth, M. Rombouts, D.M. Schrijvers, W. Martinet, G.R. De Meyer, Cholesterol-independent effects of atorvastatin prevent cardiovascular morbidity and mortality in a mouse model of atherosclerotic plaque rupture, Vasc. Pharmacol. 80 (2016) 50–58.
[20] A. Kurdi, W. Martinet, G.R. De Meyer, mTOR inhibition & cardiovascular diseases: Dyslipidemia and Atherosclerosis, Transplantation 102 (2018) S44–S46.
[21] H. Hartwig, C. Silvestre Roig, M. Daemen, E. Lutgens, O. Soehnlein, Neutrophils in atherosclerosis. A brief overview, Hamostaseologie 35 (2) (2015) 121–127.
[22] K.J. Woollard, F. Geissmann, Monocytes in atherosclerosis: subsets and functions, Nat. Rev. Cardiol. 7 (2) (2010) 77–86.
[23] P.Y. Lee, D.B. Sykes, S. Ameri, D. Kalaitzidis, J.F. Charles, et al., The metabolic regulator mTORC1 controls terminal myeloid differentiation, Sci. Immunol. 2 (11) (2017) eaam6641.
[24] C.S. Moran, R.J. Jose, J.V. Moxon, A. Roomberg, P.E. Norman, et al., Everolimus limits aortic aneurysm in the apolipoprotein E-deficient mouse by downregulating C-C chemokine receptor 2 positive monocytes, Arterioscler. Thromb. Vasc. Biol. 33 (4) (2013) 814–821.
[25] B. Ran, M. Li, Y. Li, Y. Lin, W. Liu, et al., Everolimus (RAD001) inhibits the proliferation of rat vascular smooth muscle cells by up-regulating the activity of the p27/kip1 gene promoter, Anatol. J. Cardiol. 16 (6) (2016) 385–391.
[26] M.C. Lavigne, J.L. Grimsby, M.J. Eppihimer, Antirestenotic mechanisms of everolimus on human coronary artery smooth muscle cells: inhibition of human coronary artery smooth muscle cell proliferation, but not migration, J. Cardiovasc. Pharmacol. 59 (2) (2012) 165–174.
[27] J. Aono, E. Ruiz-Rodriguez, H. Qing, H.M. Findeisen, K.L. Jones, et al., Telomerase Inhibition by Everolimus Suppresses Smooth Muscle Cell Proliferation and Neointima Formation through Epigenetic Gene Silencing, JACC Basic Transl. Sci. 1 (1–2) (2016) 49–60.
[28] E.M. Rzucidlo, K.A. Martin, R.J. Powell, Regulation of vascular smooth muscle cell differentiation, J. Vasc. Surg. 45 (2007) (Suppl A:A25-32).
[29] S. Verheye, W. Martinet, M.M. Kockx, M.W. Knaapen, K. Salu, et al., Selective clearance of macrophages in atherosclerotic plaques by autophagy, J. Am. Coll. Cardiol. 49 (6) (2007) 706–715.
[30] J.F. Bentzon, F. Otsuka, R. Virmani, E. Falk, Mechanisms of plaque formation and rupture, Circ. Res. 114 (12) (2014) 1852–1866.
[31] D.A. Chistiakov, A.N. Orekhov, Y.V. Bobryshev, Contribution of neovascularization and intraplaque haemorrhage to atherosclerotic plaque progression and instability, Acta Physiologica (Oxford, England). 213 (3) (2015) 539–553.
[32] S. Wang, K.R. Amato, W. Song, V. Youngblood, K. Lee, et al., Regulation of endothelial cell proliferation and vascular assembly through distinct mTORC2 signaling pathways, Mol. Cell. Biol. 35 (7) (2015) 1299–1313.
[33] E. Paoletti, mTOR inhibition and cardiovascular diseases: cardiac hypertrophy, Transplantation 102 (2S) (2018) S41–s43 Suppl 1.
[34] A. Uchinaka, M. Yoneda, Y. Yamada, T. Murohara, K. Nagata, Effects of mTOR inhibition on cardiac and adipose tissue pathology and glucose metabolism in rats with metabolic syndrome, Pharmacol. Res. Perspect. 5 (4) (2017) e00331.
[35] T. Imamura, K. Kinugawa, D. Nitta, O. Kinoshita, K. Nawata, et al., Everolimus Attenuates Myocardial Hypertrophy and Improves Diastolic Function in Heart Transplant Recipients, Int. Heart J. 57 (2) (2016) 204–210.
[36] E. Paoletti, L. Marsano, D. Bellino, P. Cassottana, G. Cannella, Effect of everolimus on left ventricular hypertrophy of de novo kidney transplant recipients: a 1 year, randomized, controlled trial, Transplantation 93 (5) (2012) 503–508.